Local environment surrounding Co in MBE-grown Co-doped HfO$_2$ thin films probed by EXAFS

Y. L. Soo, S. C. Weng, W. H. Sun, S. L. Chang, W. C. Lee, Y. S. Chang, J. Kwo, and M. Hong
Department of Physics and Department of Materials Science and Engineering, National Tsing Hua University, Hsinchu 30013, Taiwan

J. M. Ablett and C.-C. Kao
National Synchrotron Light Source, Brookhaven National Laboratory, Upton, New York 11973, USA

D. G. Liu and J. F. Lee
National Synchrotron Radiation Research Center, Hsinchu 30013, Taiwan

Local structure around Co impurity atoms in HfO$_2$:Co thin films prepared by molecular beam epitaxy has been investigated using the extended x-ray absorption fine structure (EXAFS) technique. These films were found to be ferromagnetic at room temperature. Progressive formation of Co clusters was observed accompanied by interstitial doping of Co in samples with Co concentration of 1%–20% grown at a substrate temperature of ~700 °C. However, films with a relatively high Co concentration of ~10% can be prepared without clustering of Co metal in a low-temperature growth mode with a substrate temperature ~100 °C. These low-temperature-grown films were found to be thermally stable up to an annealing temperature of ~700 °C. Our EXAFS results have therefore verified the feasibility for preparing Co-cluster-free room-temperature-ferromagnetic HfO$_2$:Co-diluted magnetic oxide thin films with great potential for possible spintronic applications.

PACS number(s): 61.10.Ht

I. INTRODUCTION

The high-k oxide HfO$_2$, with a dielectric constant 5 times larger than that of SiO$_2$, has been considered one of the most promising insulators useful for resolving the tunneling problem in semiconductor devices as its size is reduced and approaches the quantum mechanical limit. In addition to its great potential as a next-generation insulator, HfO$_2$ thin films are also reported to exhibit ferromagnetism without magnetic dopants[1] and to be one of several oxide matrices that can largely enhance the magnetic moment of transition-metal dopant atoms such as Co at room temperature.[2] In light of the outstanding dielectric and magnetic properties of Co-doped HfO$_2$, it is conceivable that spintronic devices with nanometer size and spin polarization capability can be developed by making use of this material system. Apart from the potential technological applications, the mechanism underlying the reported enhancement of the magnetic moment in these materials is also a very intriguing scientific question that deserves a detailed investigation.

To understand the magnetic behavior of the HfO$_2$:Co system, the location of Co impurity atoms in the HfO$_2$ host oxide is a crucially important prerequisite. Of special importance, the possibility of clustering of Co metal in the samples for magnetic measurements may consequently mislead the data interpretation and therefore has to be ruled out beforehand. To this end, we have employed the extended x-ray absorption fine structure (EXAFS) technique to probe the local structures around Co atoms in Co-doped HfO$_2$ of different Co concentrations grown by a state-of-the-art molecular beam epitaxy (MBE) method at different growth temperatures. Since the Co dopant atoms in either the HfO$_2$ matrix or the Co clusters in general lack long-range structural order, the short-range-order EXAFS method is therefore uniquely suited for locating Co atoms in the oxide matrix, as well as monitoring possible Co cluster formation, in these MBE-grown samples.

II. EXPERIMENT

Thin films of HfO$_2$:Co with a thickness of 120 nm were grown by MBE on yittrium-stabilized zirconia (YSZ) substrates at a high temperature 700 °C and a low temperature 100 °C. The Co concentration was estimated based on molecular flow and growth rate to be 1, 2, 4, and 20 at. % for the high-temperature-grown samples TH288, TH287, TH264, and TH262, respectively. The Co concentration in the low-temperature-grown sample TH398 was determined to be 10 at. % using the same method. All the samples investigated in this work were found to be ferromagnetic at room temperature by superconducting quantum interference device (SQUID) measurements. Extensive magnetic analysis as well as transmission electron microscopy (TEM) structural analysis is demonstrated in another paper.[3] The average short-range-order structures around the magnetic Co dopants were probed by Co K-edge EXAFS. The x-ray absorption measurements were performed in conventional fluorescence mode at beamline BL01C of National Synchrotron Radiation Research Center (NSRRC) and beamline X27A[4] of the National Synchrotron Light Source at Brookhaven National Laboratory using a single-element Si(Li) detector and a 13-element Ge detector at room temperature, respectively. Detailed experimental procedures can be found in some of our previous papers.[5–9] To study the thermal stability of the low-temperature-grown sample, sample TH398 was annealed at 350 °C and 700 °C and Co K-edge EXAFS were measured after each annealing.

To obtain local structural information of Co in the samples, the EXAFS χ functions were extracted from the raw experimental data using a well-established data reduction process.[9,10] The χ as a function of photoelectron momentum (k) was truncated and Fourier transformed to real (R) space. The first pronounced peak in R space representing the nearest-neighboring shells surrounding the central Co at-

TABLE I. Parameters of local structure around Co atoms obtained from curve fitting of the Co K-edge EXAFS. The amplitude reduction factor S_0^2 representing the central atom shake-up and shake-off effects was determined in a previous paper.[a] N is the coordination number. R is the bond length. σ^2 is the Debye-Waller-like factor serving as a measure of local disorder. ΔE_0 is the difference between the zero kinetic energy value of the sample and that of the theoretical model used in FEFF. Underlined values were kept constant during the iterative fitting process. Uncertainties were estimated by the double-minimum residue ($2\chi^2$) method.

Sample	Neighboring atom	N	R (Å)	σ^2 (10^{-3} Å^2)	ΔE (eV)	S_0^2
TH264	O	1.0±0.7	2.06±0.04	$\underline{6}$	7±11	$\underline{0.7}$
	Co	5.5±0.8	2.49±0.01	6±2	−1±4	
TH262	O	1.7±0.5	$\underline{2.06}$	2±5	9±7	$\underline{0.7}$
	Co	6.7±0.9	2.49±0.02	10±2	0±4	
TH287	O	2.8±0.9	$\underline{2.06}$	$\underline{9}$	8±4	$\underline{0.7}$
	Co	4.9±1.4	2.48±0.02	9±3	1±4	
TH288	O	2.0±0.3	2.04±0.01	4±3	4±5	$\underline{0.7}$
	Co	3.8±0.4	2.49±0.01	14±1	2±5	
TH398 As-grown	O	3.8±0.2	1.97±0.01	10±1	−5±1	$\underline{0.7}$
TH398 350 °C annealed	O	3.7±0.1	1.88±0.01	9±1	−12±1	$\underline{0.7}$
TH398 700 °C annealed	O	2.5±0.2	1.91±0.01	1±1	−11±5	$\underline{0.7}$
	Hf	1.6±0.4	2.56±0.02	6±3	12±3	

[a]See Ref. 6.

oms was selected and back transform to the k space. Such Fourier-filtered function was then curve fitted with theoretical backscattering amplitude and phase-shift functions calculated by the FEFF program.[11,12] The local structural parameters determined by curve fittings are listed in Table I. In the curve-fitting process, a k range of 3.0–9.85 Å^{-1} was adopted for all samples and an R range of 1.32–2.76 Å was selected for TH287 and 1.06–2.92 Å for all other samples. The degrees of freedom for the Fourier-filtered spectra is thus estimated to be 8–10,[13] which is sufficient for extracting all the fitting parameters in Table I from the Fourier-filtered data. The experimental EXAFS χ functions and Fourier transforms of the high-temperature-grown and low-temperature-grown samples are plotted with their respective theoretical curve from curve fittings in Figs. 1 and 2, respectively. As a complementary support to our EXAFS analysis, the x-ray-absorption near-edge structures (XANES) for all four high-temperature-grown samples were isolated from the raw absorption spectra and plotted in Fig. 3 for comparison with that of the low-temperature-grown sample. All the XANES spectra have been normalized to the height of the first peak above the absorption edge.

III. RESULTS AND DISCUSSION

As shown in Fig. 1, the Fourier transforms of samples TH287, TH262, and TH264 grown at 700 °C with Co concentration ranging from 2% to 20% exhibit only one pronounced first peak near 2.0 Å. On the other hand, the corresponding "first peak" of sample TH288 also grown at

700 °C but with the lowest Co concentration of 1% is actually composed of two largely overlapped peaks. Curve-fitting results shown in Table I indicate that the two overlapped peaks in the Fourier transform of TH288 are due to an O neighboring shell and a Co shell with coordination numbers 2.0±0.3 and 3.8±0.4 at distances of 2.04±0.01 Å and
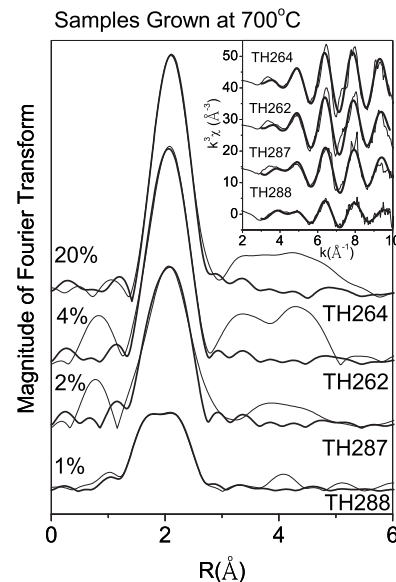

FIG. 1. Fourier transform of Co K-edge EXAFS χ functions for samples grown at ~700 °C. Thin lines: experiment. Thick lines: theoretical. Inset: weighted Co K-edge EXAFS χ functions. Curves have been shifted vertically for the sake of clarity.
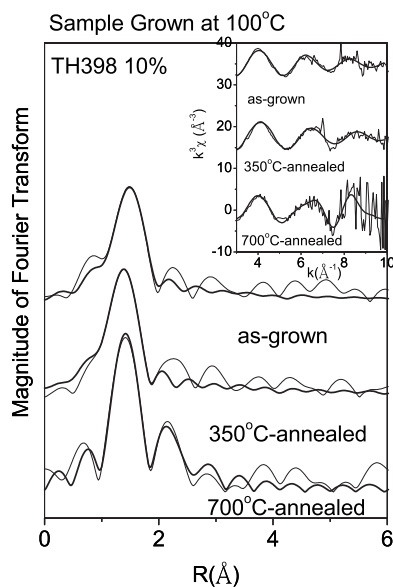
FIG. 2. Fourier transform of Co K-edge EXAFS χ functions for the sample grown at $\sim 100\,^{\circ}\text{C}$. Thin lines: experiment. Thick lines: theoretical. Inset: weighted Co K-edge EXAFS χ functions. Curves for the as-grown and $350\,^{\circ}\text{C}$–annealed samples have been shifted vertically for the sake of clarity.

2.49 ± 0.01 Å from the central Co atom, respectively. Since the Co-O bond length in this sample is appreciably shorter than the Hf-O bond length 2.22 Å in HfO_2 and the Co-O bond length 2.13 Å in CoO, we infer that Co atoms neither substitute for Hf nor form a CoO second phase. Our results suggest that some Co dopant atoms are most likely located at an interstitial site in the HfO_2 matrix while others form Co clusters as indicated by the existence of the Co shell. The curve-fitting parameters shown in Table I have further revealed that the O shell and Co shell are both present also in samples of higher Co concentration, indicating coexistence of interstitially doped HfO_2:Co and Co clusters in those samples. However, the ratio of Co to O has increased from 1.9 and 1.8 to 3.9 and 5.5 as the Co concentration increases from 1% and 2% to 4% and 20%, respectively. Owing to the increased coordination number and decreased disorder represented by the Debye-Waller-like factor σ^2 in the Co shell, the relatively weak O peak has merged into the increasingly dominant Co peaks in the Fourier transform of samples with higher Co concentration. The EXAFS results demonstrate that progressive formation of Co clusters has taken place in the high-temperature-grown samples as the Co concentration increases in these samples.

The EXAFS data of sample TH398 with a relative high Co concentration of 10% grown at a much lower temperature of $100\,^{\circ}\text{C}$ appear to be very different from those of the $700\,^{\circ}\text{C}$–grown samples. As shown in Fig. 2 and Table I, only one pronounced peak corresponding to an O neighboring shell of coordination number 3.8 ± 0.2 at a distance of 1.97 ± 0.01 Å appears in the Fourier transform of the as-grown sample. In comparison, the distance of the O shell is appreciably shorter than that of the $700\,^{\circ}\text{C}$–grown samples and no Co shell is observed in the $100\,^{\circ}\text{C}$–grown sample. If Co clusters were also present in this low-temperature-grown
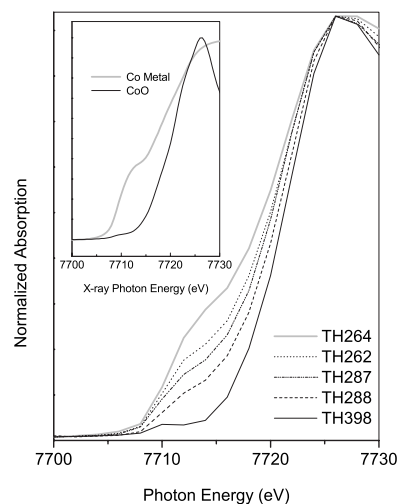

FIG. 3. Normalized x-ray absorption near the Co K absorption edge for HfO_2:Co samples. Inset: normalized x-ray absorption near the Co K absorption edge for Co metal and CoO model compound.

sample, we would expect the Co near-neighboring shell around the central Co atom to appear close to the O shell similar to the case of high-temperature-grown samples discussed above. However, introducing such a Co shell into the local structural model for this sample always results in a negligible coordination number for that shell in our curve fitting. The absence of a Co near-neighboring shell in the EXAFS data indicates that the low-temperature-grown sample is nearly free of Co clusters in comparison to the obvious Co-cluster formation in the high-temperature-grown samples. After annealing at $350\,^{\circ}\text{C}$, the distance of the O shell is decreased to 1.88 ± 0.01 Å while its coordination number remains roughly the same as that of the as-grown sample. However, in the Fourier transform of the $700\,^{\circ}\text{C}$-annealed sample, a second peak best-fitted as 1.6 ± 0.4 Hf at 2.56 ± 0.02 Å seems to emerge from the noise level in addition to the O shell of a slightly lowered coordination number 2.5 ± 0.2 and a distance 1.91 ± 0.01 Å. It is worth noting that our EXAFS analysis has found no sign of Co cluster formation in the $100\,^{\circ}\text{C}$–grown sample even after annealing at an elevated temperature of $700\,^{\circ}\text{C}$. In contrast to the apparent Co cluster formation in the high-temperature-grown samples, our EXAFS analysis has found no Co cluster in the low-temperature-grown sample.

As a complementary support to our EXAFS analysis, the XANES data can be employed to confirm the progressive formation of Co clusters in the high-temperature-grown samples, as well as the absence of Co clusters in the low-temperature-grown sample. The near-absorption-edge features appearing in a XANES spectrum reflect the density of unoccupied states near the Fermi level and therefore can be used to monitor the local structural variation among samples prepared under different growth conditions. As shown in the inset of Fig. 3, the XANES of Co metal with Co in a Co-coordinated local environment is distinctly different from that of the CoO model compound in which Co is surrounded by O nearest-neighboring atoms. Most significantly, the shoulder feature appearing at around 7710 eV in the spectrum for Co metal is absent from that of CoO. The XANES

of the low-temperature-grown TH398 largely resemble that of CoO; this is consistent with the EXAFS result that Co atoms in TH398 are surrounded by O nearest-neighboring atoms. On the other hand, the shoulder feature at around 7710 eV representing the Co metal/cluster component shows up in the XANES of the high-temperature-grown samples and its intensity increases with increasing Co concentration of 1%, 2%, 4%, and 20% for samples TH288, Th287, Th262, and TH264, respectively. This observation is also consistent with the progressive formation of Co clusters in the high-temperature-grown samples revealed by the EXAFS analysis.

As a side remark, although the XANES analysis has qualitatively confirmed the EXAFS results, it appears somewhat difficult to obtain a reliable quantitative analysis for the XANES data in the present work. In the XANES regime, features arising from electronic structure can be largely mixed with EXAFS oscillations. Separation of the EXAFS and XANES features in the near-edge regime appears to be a formidable task for the present work due to the limited energy resolution in our hard-x-ray measurements and the lack of knowledge of the three-dimensional structure around Co dopant atoms in these material systems. Therefore, we have used the XANES spectra to qualitatively confirm our EXAFS results and extracted all our quantitative structural information exclusively from the later.

In light of the distinct local structural difference around Co revealed by our EXAFS analysis, we can see that the selection of growth temperature is crucially important for preparing HfO_2:Co samples for studying their reported magnetic properties. Progressive formation of Co clusters observed in samples grown at elevated temperatures ~ 700 °C, commonly used in the MBE processes, can dominantly affect the data of magnetic measurements and thus lead to incorrect conclusion. On the other hand, samples prepared using unusually low growth temperature of ~ 100 °C are found to be free of Co clusters and therefore are worth further investigation. The TEM and magnetic measurements demonstrated in Ref. 3 have revealed that the clusterlike image and superparamagnetism are present in the high-temperature-grown samples but absent from the low-temperature-grown samples. These are consistent with our EXAFS results, that the low-temperature-grown sample is nearly Co cluster free

and Co clusters are formed in the high-temperature-grown samples. Furthermore, the magnetic moment per Co in the low-temperature-grown samples is found to be in the same order of that in the high-temperature-grown samples. Therefore, the ferromagnetism in the low-temperature-grown sample is most likely due to intrinsic magnetism of HfO_2:Co, instead of any possible Co clusters too dilute to be detected by EXAFS. It is remarkable that the Co-cluster-free samples are ferromagnetic at room temperature, making this material system one of the ferromagnetic-diluted magnetic oxides largely interested in for possible spintronic applications.

IV. CONCLUSIONS

Our EXAFS data have indicated that HfO_2:Co films with relatively high Co concentration ~ 10 at. % can indeed be prepared free of Co clustering in an MBE process with low growth temperature of ~ 100 °C. The formation of Co clusters in such a low-temperature-grown HfO_2:Co films is somehow inhibited even after annealing at elevated temperatures up to 700 °C. By contrast, growth of the film at 700 °C inevitably leads to progressive formation of Co clusters even at a Co concentration as low as 1 at. %. More experimental work has to be performed to understand the magnetic properties of the Co doped HfO_2 system. In any case, clustering of magnetic Co metal in the samples has to be avoided to prevent misinterpretation of the experimental data. As revealed by our x-ray results, the seemly inevitable formation of Co clusters under regular MBE growth mode with a growth temperature ~ 700 °C can indeed be deterred to achieve cluster-free HfO_2:Co films by using a much lower growth temperature ~ 100 °C. The low-temperature-grown films are therefore verified to be a ferromagnetic-diluted magnetic oxide with great potential in possible spintronic applications.

ACKNOWLEDGMENTS

[1] M. Venkatesan, C. B. Fitzgerald, and J. M. D. Coey, Nature (London) **430**, 630 (2004).

[2] M. S. Ramachandra Rao, S. Dhar, S. J. Welz, S. B. Ogale, Darshan C. Kundaliya, S. R. Shinde, S. E. Lofland, C. J. Metting, R. Erni, N. D. Browning, and T. Venkatesan (unpublished).

[3] Y. H. Chang, Y. L. Soo, S. F. Lee, W. C. Lee, M. L. Huang, M. J. Lee, S. C. Weng, W. H. Sun, J. M. Ablett, C.-C. Kao, M. Hong, and J. Kwo, Appl. Phys. Lett. **91**, 082504 (2007).

[4] J. Ablett, C. Kao, R. Reeder, Y. Tang, A. Lanzirotti, Nucl. Instrum. Methods Phys. Res. A **562** 487 (2006).

[5] Y. L. Soo, G. Kioseoglou, S. Kim, S. Huang, Y. H. Kao, S. Kuwabara, S. Owa, T. Kondo, and H. Munekata, Appl. Phys. Lett. **79**, 3926 (2001).

[6] Y. L. Soo, G. Kioseoglou, S. Kim, Y. H. Kao, P. Sujatha Devi, John Parise, R. J. Gambino, and P. I. Gouma, Appl. Phys. Lett. **81**, 655 (2002).

[7] Y. L. Soo, G. Kioseoglou, S. Kim, X. Chen, H. Luo, Y. H. Kao, Y. Sasaki, X. Liu, and J. K. Furdyna, Appl. Phys. Lett. **80**, 2654 (2002).

[8] Y. L. Soo, S. Wang, S. Kim, G. Kim, M. Cheon, X. Chen, H. Luo, Y. H. Kao, Y. Sasaki, X. Liu, and J. K. Furdyna, Appl. Phys. Lett. **83**, 2354 (2003).

[9] Y. L. Soo, Z. H. Ming, S. W. Huang, Y. H. Kao, R. N. Bhargava, and D. Gallagher, Phys. Rev. B **50**, 7602 (1994), and references cited therein.

[10] M. Newville, P. Līvins, Y. Yacoby, J. J. Rehr, and E. A. Stern, Phys. Rev. B **47**, 14126 (1993).

[11] P. A. Lee, P. H. Citrin, P. Eisenberger, and B. M. Kincaid, Rev. Mod. Phys. **53**, 769 (1981).

[12] J. J. Rehr, J. Mustre de Leon, S. I. Zabinsky, and R. C. Albers, J. Am. Chem. Soc. **113**, 5135 (1991).

[13] E. A. Stern, Phys. Rev. B **48**, 9825 (1993).